Large-Scale Modes of a Non-Rotating Atmosphere with Water Vapor and Cloud-Radiation Feedbacks

Željka Fuchs and David J. Raymond*

Physics Department and Geophysical Research Center

New Mexico Tech

Socorro, NM 87801

USA

Revised version submitted to *J. Atmos. Sci.*

October 18, 2005

*Corresponding author; raymond@kestrel.nmt.edu, currently on sabbatical leave at Centro de Ciencias de la Atmósfera, Universidad Autónoma Nacional de México.

Abstract

A minimal model of a moist equatorial atmosphere is presented in which the precipitation rate is assumed to depend on just the vertically averaged saturation deficit and the convective available potential energy. When wind induced surface heat exchange (WISHE) and cloud-radiation interactions are turned off, there are no growing modes. Gravity waves with wavenumbers smaller than a certain limit respond to a reduced static stability due to latent heat release, and therefore propagate more slowly than dry modes, while those with larger wavenumbers respond to the normal dry static stability. In addition, there exists a stationary mode which decays slowly with time. For realistic parameter values, the effect of reduced static stability on gravity waves is limited to wavelengths greater than the circumference of the earth. WISHE and cloud-radiation interactions both destabilize the stationary mode, but not the gravity waves.

1 Introduction

Moist convection, surface fluxes, and radiation play a fundamental role in the large-scale dynamics of the tropical atmosphere to a much greater degree than in middle latitudes. Many attempts have been made to characterize this role in simplified models. These models fall into two broad categories, convergence-driven models and quasi-equilibrium models.

- Convergence-driven models: Convection in models of this type is driven either by low-level mass convergence or moisture convergence. Variations on such models are legion, but early examples are the models of Yamasaki (1969), Hayashi (1971), Lindzen (1974). Following Lindzen's terminology, these are generally called wave-CISK models, where CISK stands for conditional instability of the second kind (Charney and Eliassen, 1964). Such models are currently looked upon with disfavor for a variety of reasons. In particular, they ignore surface energy fluxes and variations in tropospheric humidity, the effects of which tend to be stronger than the effects of large-scale convergence in driving convection. They also tend to produce modes with the largest growth rates at the smallest scales, contrary to the original expectation of explaining large-scale tropical dynamics.

- Quasi-equilibrium models: Starting with Emanuel's (1987) model of the Madden-Julian oscillation (Madden and Julian, 1971, 1972, 1994; see also Yano and Emanuel, 1991; Emanuel 1993), a series of models have been proposed which invoke the notion that deep convection exists in a state of near-equilibrium with the processes which destabilize the tropical environment to convection. This idea owes its origin to Arakawa and Schubert (1974). A noteworthy model of this type is that proposed by Neelin and Yu (1994). This model uses a simplified version of the Betts-Miller cumulus parameterization to treat convection (Betts, 1986; Betts and Miller, 1986; Betts and Miller, 1993). This parameterization implements a form of convective adjustment, which is a type of quasi-equilibrium model. Typically, in

models of this type, unstable modes do not occur unless helped along by some process beyond free tropospheric dynamics, such as spatially varying surface energy fluxes.

Interestingly, the above model types consider deep convection and surface latent and sensible heat fluxes, but typically ignore the possibility that radiation might play more of a role than that of a uniformly distributed energy sink. However, recently numerical models have demonstrated the key effects of cloud-radiation interactions in modulating, and possibly even driving large-scale disturbances in the tropics (Slingo and Slingo, 1988, 1991; Randall, Harshvardhan, Dazlich, and Corsetti 1989; Sherwood, Ramanathan, Barnett, Tyree, and Roeckner, 1994; Raymond, 2000a, 2001). Basically, middle to upper level stratiform cloudiness produced by deep convection reduces outgoing longwave radiation (OLR) to space, resulting in differential heating between cloudy and clear regions, which tends to reinforce the pre-existing convection. This effect may be strong enough to destabilize otherwise stable large-scale modes. Raymond (2001) proposed that cloud-radiation interactions are a primary driver of the Madden-Julian oscillation.

The convective quasi-equilibrium hypothesis by itself provides an incomplete description of tropical convection (Emanuel, Neelin, and Bretherton, 1994). Needed in addition is a model of how convection reacts to variations in the humidity of the atmosphere. The Betts-Miller cumulus parameterization postulates a very simple model in this regard. If the column-integrated water vapor exceeds that required to produce a target relative humidity profile, the excess is removed as precipitation over a period of a few hours. If it is less than needed, deep convection is turned off in favor of a shallow, non-precipitating convection scheme. Other quasi-equilibrium models such as the Arakawa-Schubert scheme (Arakawa and Schubert, 1974) are typically more complex in their behavior, but nevertheless react systematically in some way to varying humidity profiles.

Raymond (2000b) proposed a particularly simple relationship between humidity and precipitation over warm tropical oceans, namely that the precipitation rate is inversely

proportional to the vertically averaged saturation deficit. This hypothesis is clearly an oversimplification, but is roughly borne out by observation. For instance, figure 1 shows a scatter plot of the monthly averaged values of precipitation rate and column water vapor within 20° of the equator. Since the temperature profile in the tropics is nearly the same everywhere, the column water vapor is just a constant minus the vertically integrated saturation deficit. Though significant scatter exists, there is clearly a relationship between the column water vapor and the precipitation rate in this figure. (The correlation may or may not be weaker on daily time scales. This issue remains to be explored.)

In all likelihood, the precipitation rate depends also on the convective available potential energy (CAPE), though the nature of this dependence is considerably less certain than the dependence on saturation deficit.

The Betts-Miller cumulus parameterization is an example of a parameterization in which the precipitation rate is largely determined by the saturation deficit and the CAPE. The saturation deficit dependence is straightforward — column water vapor in excess of that which corresponds to a certain mean relative humidity is precipitated out on a time scale of a few hours.

The dependence of precipitation on CAPE is a bit more subtle. The usual causes of a CAPE value in excess of the equilibrium value prescribed by the parameterization are a decrease in the temperature of the middle troposphere or an increase in the moist static energy of the boundary layer. The parameterization responds in both cases by adjusting the target temperature profile over a period of a few hours to restore the target CAPE value. If the cause of the CAPE perturbation is excess moisture in the boundary layer, this moisture is mixed through the depth of the troposphere, and then precipitated out by the humidity relaxation process. On the other hand, a decrease in mid-tropospheric temperature increases the relative humidity, triggering additional precipitation as well. In both cases, increased CAPE results indirectly in increased precipitation, though the amount depends on the mechanism of CAPE increase.

The purpose of this paper is to develop a minimal model of the interaction between precipitation, radiation, surface fluxes, and free tropospheric tropical dynamics. In order to simplify the treatment as much as possible, rotation is omitted. This may be less restrictive than it first appears, because the zonal dynamics of equatorial Kelvin waves are identical to those of gravity waves in a non-rotating environment. An additional assumption is that all disturbances have a sinusoidal vertical structure with a vertical wavelength equal to that of the gravest mode in the tropical troposphere. If Mapes (1993, 2000) is correct, this may constitute a serious over-simplification, but we feel justified in using it in our initial attempt at a minimal model. An additional consequence of this assumption is that no heating or moistening can occur at the surface. This would be a problem in models establishing the global base state, but should not be a serious limitation for disturbances of the type being studied here.

The key hypothesis of the model is that the precipitation rate depends only on the vertically averaged saturation deficit and the CAPE. In the context of the linearization and the vertical mode truncation, this reduces to a dependence of the precipitation perturbation on the tropospheric temperature and humidity perturbations, where the base state is one of radiative-convective equilibrium. As we shall see, the large-scale dynamics of the model depends critically on the sensitivity of precipitation rate to these perturbations.

2 Model and analytical solutions

Our model is Boussinesq and non-rotating with a rigid lid at the tropopause. The hydrostatic governing equations are linearized about a state of rest and radiative-convective equilibrium, and highly simplified thermodynamics are invoked so as to make the solution of the model equations analytically tractable. The omission of rotation eliminates most tropical disturbances, leaving gravity waves as the only free modes. The rigid lid is a significant over-simplification, but is justifiable in the present context.

2.1 Linearized governing equations

The linearized governing equations used in the model are the horizontal momentum equation, the hydrostatic equation, mass continuity, and equations for scaled versions of the potential temperature, mixing ratio, and equivalent potential temperature:

$$\frac{\partial u}{\partial t} + \frac{\partial p}{\partial x} = 0 \tag{1}$$

$$\frac{\partial p}{\partial z} = b \tag{2}$$

$$\frac{\partial u}{\partial x} + \frac{\partial w}{\partial z} = 0 \tag{3}$$

$$\frac{\partial b}{\partial t} + \Gamma_B w = s_B \tag{4}$$

$$\frac{\partial q}{\partial t} + \Gamma_Q w = s_Q \tag{5}$$

$$\frac{\partial e}{\partial t} + \Gamma_E w = s_E \tag{6}$$

The horizontal and vertical wind components are u and w, the kinematic pressure perturbation is p, and $b = g\theta'/\theta_0$, where g is the acceleration of gravity, θ' is the perturbation from a reference profile of potential temperature $\theta_0(z)$. The quantity

$$\Gamma_B = \frac{g}{\theta_0}\frac{d\theta_0}{dz} \tag{7}$$

is the square of the Brunt-Väisälä frequency.

Equations (5) and (6) are inspired by an approximate expression for the equivalent potential temperature:

$$\theta_e \approx \theta \exp[Lr/(C_p T_{ref})] \approx \theta \left(1 + \frac{Lr}{C_p T_{ref}}\right) \approx \theta + \frac{Lr}{C_p}, \tag{8}$$

where r is the mixing ratio, L is the latent heat of evaporation, C_p is the specific heat of air at constant temperature, and T_{ref} is a constant reference temperature. In the last of the series of approximations in the above equation we have set $\theta \approx T_{ref}$ in the mixing ratio term. Multiplying this equation by g/θ_0 and defining $e = g\theta'_e/\theta_0$ and

$q = gLr'/(C_p\theta_0)$, where θ'_e and r' are deviations from reference profiles θ_{e0} and r_0, we find that

$$e = b + q. \tag{9}$$

Furthermore, since $\theta_{e0} = \theta_0 + Lr_0/C_p$, we have

$$\Gamma_E = \Gamma_B + \Gamma_Q \tag{10}$$

where

$$\Gamma_E = \frac{g}{\theta_0}\frac{d\theta_{e0}}{dz} \qquad \Gamma_Q = \frac{gL}{C_p\theta_0}\frac{dr_0}{dz}. \tag{11}$$

Thus,

$$s_E = s_B + s_Q. \tag{12}$$

One of the three equations (4), (5), and (6) is redundant, which we take to be (6).

2.2 Thermodynamic assumptions

Let us first solve (1) - (5) for the special case in which $s_B = 0$ and Γ_B is constant, with rigid horizontal surfaces at $z = 0, h$. Assuming that all dependent variables are proportional to $\exp[i(kx - \omega t)]$, we easily find free gravity wave solutions with

$$(w, b, q) = (W, B, Q)\sin(n\pi z/h) \tag{13}$$

and

$$(u, p) = (U, \Pi)\cos(n\pi z/h), \tag{14}$$

where n is a positive integer. The dispersion relation is $\omega^2 = k^2\Gamma_B/m^2$ where $m = n\pi/h$ is the vertical wavenumber. Further development will be limited to consideration of the fundamental vertical mode ($n = 1$).

We take $h = 15$ km, the approximate depth of the tropical troposphere, so that the vertical wavenumber for the fundamental mode is $m = \pi/h \approx 2 \times 10^{-4}$ m^{-1}.

Let us suppose that s_B, s_Q, and s_E all have the vertical structure of the fundamental mode of the above adiabatic solution, i. e., are proportional to $\sin(mz)$, where $m = \pi/h$:

$$(s_B, s_Q, s_E) = (S_B, S_Q, S_E)\sin(mz). \tag{15}$$

This assumption is weak in the sense that, contrary to observation, moisture perturbations do not occur at the surface. However, the assumption is necessary to maintain the simplicity of our approach to the problem.

We note that

$$\int_0^h s_B dz = \frac{2S_B}{m} = P - R \tag{16}$$

and

$$\int_0^h s_Q dz = \frac{2S_Q}{m} = E - P \tag{17}$$

where P, E, and R are scaled perturbations in the precipitation rate, the surface evaporation rate, and the vertically integrated radiative cooling rate. We further assume that turbulent motions within clouds vertically distribute the effects of latent heat release, evaporation, and radiative cooling so that their vertical structure is that of the above-defined fundamental mode. Surface sensible heat fluxes are ignored, an assumption which is reasonable over the tropical oceans, since they are typically a small fraction of the latent heat fluxes there.

Following Raymond (2000b), we assume that the precipitation rate is inversely proportional to the vertically averaged saturation deficit. A linearized version of this expressed in terms of the variables of the present model translates to $P \propto Q$. In addition, we assume that increased CAPE, represented by decreased mid-level potential temperature, results in increased precipitation. Let us express these relationships by

$$P = \alpha \int_0^h q dz - \mu \int_0^h b dz = \frac{2\alpha Q}{m} - \frac{2\mu B}{m}. \tag{18}$$

The constant α^{-1} is the time scale for the elimination of a mixing ratio anomaly by the induced precipitation anomaly. Let us call it the *moisture relaxation time*. Similarly, let us call μ^{-1} the *buoyancy relaxation time*.

An estimate for α may be obtained from an examination of figure 1. Since the precipitable water anomaly in our model is $2Q/m$, the slope of the line in figure 1 is just $\partial P/\partial(2Q/m)$. From (18) we find that

$$\alpha = \frac{\partial P}{\partial(2Q/m)} + \mu \frac{dB}{dQ}. \tag{19}$$

If there is no systematic dependence of CAPE on saturation deficit, then α is just the slope of the line relating precipitation rate to precipitable water. This slope increases with precipitable water, but a reasonable estimate might be $\alpha \approx 1$ d$^{-1} \approx 1.2 \times 10^{-5}$ s^{-1}.

Generally, moist tropical environments have smaller CAPE, i. e., larger B, than dry environments, which means that $dB/dQ > 0$. Thus, if $\mu > 0$, then α may be larger than provided by the above estimate. However, if the potential temperature of the middle troposphere increases by 1 K when the moisture increases by 2 g kg^{-1}, then $dB/dQ \approx 0.2$, and the above estimate of α may not be too far off if μ is comparable in magnitude to α.

The Betts-Miller parameterization assumes that moisture relaxation takes place in just a few hours. This would imply that $\alpha \approx (2 \text{ h})^{-1} \approx 1.4 \times 10^{-4}$ s^{-1}, or more than an order of magnitude greater than the above estimate. Thus, α is subject to significant uncertainty.

The optimal value of μ is difficult to estimate. Because of this uncertainty, we shall examine the consequences of a variety of assumptions for μ.

The bulk flux formula for surface evaporation is

$$F_q = C u_{eff} \Delta r \tag{20}$$

where Δr is the difference between the saturation mixing ratio at the sea surface temperature and the sub-cloud layer mixing ratio, $C \approx 10^{-3}$ is the transfer coefficient, and the effective wind is

$$u_{eff} = [(u_s - u_O)^2 + W^2]^{1/2}. \tag{21}$$

The constant $W \approx 3$ m s^{-1} (Miller, Beljaars, and Palmer, 1992), the sub-cloud layer wind is u_s, and the the velocity of the ocean relative to the ambient air is u_O. (We have extended the assumption of a background state at rest to one in uniform motion by working in the reference frame of the moving air, which means that the ocean is moving in the opposite direction at the ambient wind speed.)

We linearize F_q in u_s. The perturbation in F_q is

$$F_q' = C\eta u_s \Delta r \tag{22}$$

where $\eta = -u_O/u_{eff}$. We have ignored possible fluctuations in Δr, since these are not allowed by the assumed vertical distribution of the moisture perturbation.

Multiplying this equation by the scaling factor $Lg/(C_p\theta_{0s})$, where θ_{0s} is the surface value of θ_0, results in

$$E = C\eta U \Delta q \tag{23}$$

where u_s has been equated to U and where $\Delta q = Lg\Delta r/(C_p\theta_{0s})$.

An estimate of the radiative cooling anomaly is somewhat more difficult to obtain, as an explicit measure of cloudiness is not part of the present model. However, cloudiness is likely to increase with mixing ratio, which would in turn decrease radiative cooling. A simple expression of this relationship could therefore be written

$$R = -\gamma \int_0^h q dz = -\frac{2\gamma Q}{m}, \tag{24}$$

where γ is a rate constant to be determined.

An indirect way to estimate γ is by relating changes in the radiative cooling to changes in the precipitation rate. Changing from no rain to 15 mm d^{-1} (the largest precipitation rate in figure 1) is likely to be associated with a change from clear to totally overcast conditions, resulting in a decrease in OLR of about 150 W m^{-2}. Since the surface longwave flux doesn't vary much with cloudiness, this decrease in OLR approximates the decrease in longwave cooling. However, according to the results of Cox and Griffith (1979), deep cloudiness also decreases shortwave heating of the atmosphere by approximately half the decrease in longwave cooling, making the net decrease in cooling about half of 150 W m^{-2}, or approximately 80 W m^{-2}.

Condensation leading to rainfall of 15 mm d^{-1} corresponds to latent heat release of about 400 W m^{-2}. Eliminating Q between (18) and (24) results in the estimate $\gamma \approx -\alpha R/P \approx (80/400)\alpha = 0.2\alpha$. We therefore assume that

$$\gamma = \epsilon\alpha, \tag{25}$$

where we take $\epsilon \approx 0.2$. We call ϵ the cloud-radiative feedback parameter. Chris Bretherton (personal communication) independently finds that $\epsilon \approx 0.15$, which lends support to our estimate.

Combining these factors leads to final expressions for the source terms for buoyancy

$$S_B = \alpha(1+\epsilon)Q - \mu B \tag{26}$$

and mixing ratio

$$S_Q = U\delta - \alpha Q + \mu B, \tag{27}$$

where $\delta = mC\eta\Delta q/2$.

A typical value for the dry static stability is $\Gamma_B = 10^{-4}$ s^{-2}. The moist static stability is given by Γ_E. Emanuel, Neelin, and Bretherton (1994) estimate that a typical value of this parameter is $\Gamma_E \approx 0.1\Gamma_B$. We will adopt this value. Using $\Gamma_E = \Gamma_B + \Gamma_Q$, we therefore find that $\Gamma_Q = -0.9\Gamma_B$.

2.3 Dispersion relation

Based on (15) - (27), we can now solve the linearized moist atmosphere problem. The dependent variables take on the same space and time dependence as for the dry problem in this case, but the dispersion relation becomes

$$\begin{aligned} \omega^3 &+ i(\alpha+\mu)\omega^2 - \left(\frac{k^2\Gamma_B}{m^2} - \gamma\mu\right)\omega \\ &- i\alpha\frac{k^2\Gamma_B}{m^2}\left(\frac{\Gamma_E + \epsilon\Gamma_Q - i\delta(1+\epsilon)m/k}{\Gamma_B}\right) = 0 \end{aligned} \tag{28}$$

while the polarization relations are

$$U = (im/k)W \tag{29}$$

$$\Pi = (im\omega/k^2)W \tag{30}$$

$$B = -(im^2\omega/k^2)W \tag{31}$$

$$Q = \frac{1}{\alpha - i\omega}\left(-\Gamma_Q - \frac{i\mu m^2\omega}{k^2} + \frac{i\delta m}{k}\right)W. \tag{32}$$

The dispersion relation may be non-dimensionalized by defining a dimensionless frequency $\Omega = \omega/\alpha$ and wavenumber $\kappa = k\Gamma_B^{1/2}/(\alpha m)$:

$$\Omega^3 + i\sigma\Omega^2 - [\kappa^2 - \epsilon(\sigma - 1)]\Omega - i\kappa^2(\Gamma - i\Lambda/\kappa) = 0, \tag{33}$$

where

$$\sigma \equiv (\alpha + \mu)/\alpha. \tag{34}$$

A dimensionless static stability which takes into account the effects of both latent heat release and cloud-radiation interactions is defined

$$\Gamma = (\Gamma_E + \epsilon\Gamma_Q)/\Gamma_B. \tag{35}$$

If we ignore the effects of radiation, then our choice of parameters makes $\Gamma = 0.1$. On the other hand, if we include radiation and set $\epsilon = 0.2$, then we find that $\Gamma = -0.1$. Physically, this means that large scale ascent causes sufficient heating via cloud-radiative feedbacks to more than overcome any residual adiabatic cooling not countered by latent heat release, resulting in reinforcement of the ascent.

Finally, the effects of wind-induced variations in surface heat fluxes are contained in the parameter

$$\Lambda = \delta(1 + \epsilon)/(\alpha\Gamma_B^{1/2}). \tag{36}$$

If we take $\Delta r \approx 6$ g kg^{-1}, then we find $\delta = 5 \times 10^{-8}\eta$ s^{-2} and $\Lambda \approx 0.5\eta$. Recalling that $\eta = -u_O/u_{eff} = -u_O/(u_O^2 + W^2)^{1/2}$, we see that $-1 < \eta < 1$. The value $\eta = 0$ occurs when the ambient wind is zero, whereas $\eta = \pm 1$ occurs for strong ambient easterly ($\eta = -1$) or westerly winds ($\eta = 1$).

The dispersion relation may be rewritten in terms of a dimensionless phase speed $\phi = \Omega/\kappa = \omega m/(k\Gamma_B^{1/2})$. Eliminating ω in favor of ϕ in (33) results in

$$\phi^3 + (i\sigma/\kappa)\phi^2 - \left[1 - \frac{\epsilon(\sigma - 1)}{\kappa^2}\right]\phi - (i/\kappa)(\Gamma - i\Lambda/\kappa) = 0. \tag{37}$$

2.4 Analytical solutions

The behavior of the model under a horizontally homogeneous relaxation toward radiative-convective equilibrium leads to a way of estimating the parameter σ. This behavior may be investigated by setting $\kappa = 0$ in (33). The resulting simplified dispersion relation is $\Omega^3 + i\sigma\Omega^2 + \epsilon(\sigma - 1)\Omega = 0$, which has the solutions

$$\Omega = 0, -i\{\sigma \pm [\sigma^2 + 4\epsilon(\sigma - 1)]^{1/2}\}/2. \tag{38}$$

Let us first consider the situation in which there are no cloud-radiation interactions, i. e., $\epsilon = 0$. In this case there are two stationary neutral modes with $\Omega = 0$, and a single stationary decaying mode with $\Omega = -i\sigma$. In dimensional terms, $\omega = \Omega\alpha = -i\sigma\alpha$ for the decaying mode. Thus, the time constant for this decay is $(\sigma\alpha)^{-1}$.

It is instructive to compare this result with the cumulus ensemble radiative-convective equilibrium calculations of Tompkins and Craig (1998). In this work the evolution toward radiative-convective equilibrium is a process with two very different time scales. The shorter time scale is of order a few days, and represents the evolution of the temperature, humidity, convective mass flux, and precipitation rate toward stable values in a manner that nearly conserves the integrated vertical profile of equivalent potential temperature. The second time scale is much longer, approximately 15 d, and represents the evolution of the vertically averaged equivalent potential temperature to equilibrium. These results have been confirmed by Xiping Zeng (personal communication) using a different cumulus ensemble model. The short adjustment time in Zeng's model is roughly 2 d.

We identify the decaying mode in the present model with with the short-time-scale relaxation in the models of Tompkins and Craig and Zeng. The long-time-scale relaxation in the cumulus ensemble model does not exist in our scheme when $\epsilon = 0$, because the vertically averaged equivalent potential temperature cannot change with time in this case. This is because radiative cooling and horizontally averaged total surface heat fluxes do not change with time, and must balance each other for consistency. Thus, the long-time-scale relaxation time in our model is infinite.

As noted above, we estimate that $\alpha^{-1} \approx 1$ d, which by itself is roughly comparable to the short time scale of Tompkins and Craig as well as that of Zeng. Since our relaxation time is $(\sigma\alpha)^{-1}$, equating it with their short time scale implies that $\sigma \approx 1$. Thus, σ values greatly exceeding unity are not consistent with the results of cumulus ensemble models, as they would cause the short-time-scale relaxation to be much shorter than indicated by cumulus ensemble computations. The constraint imposed by ensemble model results needs to be subjected to much more scrutiny. However, taken at face value, it is hard to justify the much smaller moisture adjustment times implied by the Betts-Miller cumulus parameterization.

The radiative-convective equilibrium solution in our case is unstable when $\epsilon > 0$. However, this is an artifact of the model which arises from the neglect of surface moisture anomalies. As noted above, the assumed sinusoidal vertical structure of anomaly profiles forces potential temperature and moisture anomalies to be zero at the surface. Since the surface potential temperature and mixing ratio cannot change, the domain-averaged surface heat flux cannot change in response to changes in the radiative heat loss. Thus, a domain-wide radiative heating anomaly, represented by a non-zero ϵ in the case with $\kappa = 0$, cannot be compensated by a corresponding change in surface heat fluxes, and runaway heating or cooling therefore results when $\epsilon > 0$.

This flaw in the model is serious for the long-time behavior in radiative-convective equilibrium calculations. However, it is considerably less egregious for disturbances in which wind variations are likely to dominate the variability of surface heat fluxes.

Another hint as to the behavior of the modeled disturbances is obtained when $\Gamma, \Lambda, \epsilon = 0$, which means that WISHE modes (Yano and Emanuel, 1991) and cloud-radiation interactions are turned off, and the effective static stability is zero. The dispersion relation reduces to $\phi^3 + (i\sigma/\kappa)\phi^2 - \phi = 0$ in this case, from which we find that

$$\phi = 0, [-i\sigma \pm (4\kappa^2 - \sigma^2)^{1/2}]/(2\kappa). \tag{39}$$

This solution contains a single steady, stationary mode and two other modes which

decay with time. The latter two modes propagate when $\kappa > \sigma/2$ and are stationary when $\kappa < \sigma/2$. For $\kappa \gg \sigma/2$ the decay rate becomes negligible and the dimensionless phase speed goes to $\phi \approx \pm 1$. This corresponds to the case of ordinary gravity waves of short wavelength. As the wavelength increases, these gravity waves experience decreasing phase speeds as a result of wave-convection interactions, and become increasingly damped. At long wavelengths where propagation disappears, one of the modes tends to neutral stability, whereas the other decays. In the limit of infinite wavelength, the time constant for decay is σ^{-1}. Thus, at very long wavelengths there are two nearly neutral modes and one which decays rapidly, all of which are stationary.

The transition between long wavelength and short wavelength behavior occurs at $\kappa = \kappa_1 = \sigma/2$. In dimensional terms, this corresponds to a critical wavelength

$$\lambda_1 = 2\pi/k = 2\pi\Gamma_B^{1/2}/(\kappa_1 \alpha m) = 4\pi\Gamma_B^{1/2}/(\sigma\alpha m). \tag{40}$$

For $\alpha^{-1} = 1$ d, $\sigma = 1$, and $m = \pi/(15$ km), we find $\lambda_1 = 52000$ km, which is greater than the circumference of the earth. This choice of parameters thus puts all disturbances with physically possible wavelengths in the short wavelength regime. Increasing σ or α significantly beyond the above values would decrease the critical wavelength, making the long wavelength regime physically accessible. However, given the above comparison of radiative-convective equilibrium results with those from cumulus ensemble models, it seems unlikely that λ_1 can be much shorter than the above-quoted result, at least in the context of the present model.

The dependence on κ of the real part of the phase speed and the imaginary part of the frequency (i. e., the growth rate) for $\sigma = 1$ and $\sigma = 5$ are illustrated in figures 2 and 3.

3 Numerical solutions

We solved (37) numerically using Newton's method for $0.2 \leq \kappa \leq 5$ with a variety of parameter values. Three general cases are studied, with both cloud-radiation interactions

and surface flux variations turned off (stable case), with cloud-radiation interactions turned on (radiative-convective instability case, denoted RCI), and with surface flux variations turned on (WISHE case). In addition, a combined RCI-WISHE case is examined. Solutions are obtained in each case for $\sigma = 1$ and $\sigma = 5$.

3.1 Stable case

We begin with both RCI and WISHE turned off and with a positive effective static stability, i. e., with $\Gamma = 0.1$, $\Lambda = 0$, and $\epsilon = 0$. This situation differs from that discussed in the previous section and illustrated in figures 2 and 3 only by the addition of non-zero Γ. Figures 4 and 5 show the dispersion relations in this case with $\sigma = 1$ and $\sigma = 5$, so that the results may be compared directly with those of figures 2 and 3.

The addition of an effective static stability has significant consequences only for $\kappa \leq 0.57$ for $\sigma = 1$ and $\kappa \leq 1.4$ for $\sigma = 5$. In this range two of the modes are no longer stationary, but propagate with phase speeds much less than the phase speeds of the free gravity modes of short wavelength. These modes are convectively coupled gravity waves responding to the reduced effective static stability. These moist gravity modes decay, but at a rate that goes asymptotically to zero as the wavelength increases to infinity.

Two critical transitions thus occur when an effective static stability is added. As in the case when $\Gamma = 0$, free gravity waves are limited to wavelengths less than a certain value, which we call λ_1 in agreement with the previous section. The dimensionless wavenumber for the transition from free waves to stationary modes is only a weak function of Γ, remaining near the $\Gamma = 0$ value $\kappa_1 = \sigma/2$.

A second transition occurs when $\Gamma > 0$, from stationary modes to convectively coupled gravity waves. Let us denote the wavenumber and wavelength of this transition κ_2 and $\lambda_2 = 2\pi\Gamma_B^{1/2}/(\kappa_2 \alpha m)$. Thus, three regimes exist for positive Γ, a short wavelength regime with $\lambda < \lambda_1$, an intermediate regime with $\lambda_1 < \lambda < \lambda_2$, and a long wavelength regime with $\lambda > \lambda_2$. When $\sigma = 1$, $\lambda_2 = \lambda_1$, and the intermediate regime collapses to zero size.

At short wavelengths damped gravity waves with near-free wave propagation speeds exist. At intermediate wavelengths the gravity modes become stationary and decay with time. At long wavelengths convectively coupled gravity modes exist, with phase speeds reduced from free wave phase speeds in concordance with the reduced effective static stability. These modes decay slowly, with the decay rate going asymptotically to zero as the wavelength goes to infinity.

In all regimes an additional stationary mode exists. In the short and intermediate wavelength regimes the stationary mode decays slowly, whereas in the long wavelength regime it decays rapidly.

3.2 Radiative-convective instability (RCI)

We turn on cloud-radiation interactions by setting $\epsilon = 0.2$. This has the indirect consequence of making the effective static stability negative as well, with $\Gamma = -0.1$ for our current choice of parameter values.

The dispersion relations for $\sigma = 1$ and $\sigma = 5$ are shown in figures 6 and 7. As in the case of zero effective static stability ($\Gamma = 0$: figures 2 and 3), there is no long wavelength regime and no propagating modes exist for $\lambda > \lambda_1$. The only significant difference between this case and the $\Gamma = 0$ case is that the stationary mode is unstable rather than neutral. The dimensionless growth rate is approximately 0.1 for all wavenumbers except the very longest, so disturbances will amplify with little or no scale selection. There is no significant change in the character of the gravity waves.

We call the unstable stationary modes radiative-convective instability (RCI) modes since they result from the interaction between radiation and convective cloudiness. An increase in cloudiness suppresses outgoing longwave radiation, which causes a heating anomaly, which further enhances convection and cloudiness. A decrease in cloudiness has the opposite effect.

3.3 WISHE modes

If we turn off cloud-radiation interactions and set $\Lambda = -0.4$, corresponding to $\eta = -0.8$, then WISHE instability occurs. Figures 8 and 9 show that this instability is a long wavelength phenomenon in the current model. The instability vanishes for κ exceeding about 1.5 for both $\sigma = 1$ and $\sigma = 5$. Maximum growth rates occur near $\kappa = 0.5$.

The phase speed of the WISHE instability is to the east in this case, as expected by the choice of sign for η. The largest phase speeds occur at the longest wavelengths. The phase speeds at the wavelength of maximum growth rate range between 0.3 and 0.6 times the free gravity wave speed of 50 m s^{-1}, or $15 - 30$ m s^{-1}.

Interestingly, the stationary mode in the non-WISHE case becomes a propagating unstable mode when WISHE is turned on. The original propagating modes decay, with the eastward-moving propagating mode decaying particularly strongly at small wavenumber. This appears to be in conflict with the results of Neelin and Yu (1994), who find that their analogous eastward-propagating mode becomes unstable when WISHE is introduced.

3.4 Combined RCI-WISHE modes

When both cloud-radiation interactions and WISHE are turned on, the result is much as one might expect — a common unstable mode occurs which takes on the character of a WISHE mode for small wavenumber and RCI for large wavenumber. These results are illustrated in figures 10 and 11.

4 Discussion of results

The non-dimensionalization of the present model allows the application of the results over a wide range of physical parameters. However, the constraints imposed by cumulus ensemble models suggest that $(\sigma\alpha)^{-1}$ is in the range $1 - 4$ d. In individual values of σ and α aren't well constrained by available observations or models. However, for the

examples presented in the previous two sections, the smallest plausible value of α^{-1} is 1 d if $\sigma = 1$ and 5 d if $\sigma = 5$. In either case, $\lambda_1 \approx 52000$ km, assuming that the vertical half-wavelength of disturbances equals the depth of the troposphere. Since this value exceeds the circumference of the earth, all physically possible equatorial waves must be in the short wavelength regime. This has several consequences:

- Convective coupling damps gravity waves with physically possible wavelengths, but it doesn't significantly reduce their phase speed. The regime in which gravity waves propagate more slowly than free waves in response to an effective static stability reduced by convection is not physically realizable because the wavelengths would be far too long.

- The WISHE instability exists in the model, but if the effective static stability takes on positive values in the range suggested by Emanuel, Neelin, and Bretherton (1994), i. e., $\Gamma \approx 0.1$, then WISHE instability only occurs for wavelengths exceeding $2\pi\Gamma_B^{1/2}/(\kappa_{max}\alpha m)$ where $\kappa_{max} \approx 1.5$, or about 17000 km if $\sigma = 1$ and 86000 km if $\sigma = 5$. Thus, pure WISHE modes have global-scale wavelengths for small σ and are physically unrealizable for large σ.

- RCI and the combined RCI-WISHE instability both have a dimensionless growth rate of order 0.1 for all physically realizable wavelengths with the estimates of model parameters used in this paper. For $\alpha^{-1} = 1$ d, this corresponds to an e-folding time for amplification of 10 d, whereas for $\alpha^{-1} = 5$ d, the e-folding time is 50 d.

The results of this work are in disagreement with those of Neelin and Yu (1994), in that gravity modes responding to the reduced static stability provided by deep convection occur for physically realizable wavelengths in their model. This is doubtless due to their use of the Betts-Miller cumulus parameterization, which assumes an adjustment time of ≈ 2 h rather than ≥ 1 d, as assumed in our model.

Two caveats need to be mentioned concerning the present work. First, the computations need to be extended to an equatorial beta-plane in order for comparisons to be made with, e. g., the observational results on large scale tropical modes of Wheeler and Kiladis (1999). However, given that equatorial Kelvin waves propagate at the same speed as free gravity waves of the same equivalent depth, and that the propagation speeds of all other modes typically scale with the propagation speed of Kelvin waves, it seems probable that the spectrum of convectively coupled wave modes predicted by our model on an equatorial beta plane will be more consistent with free gravity wave propagation speeds rather than the reduced speeds inferred by Wheeler and Kiladis. Work on this extension is in progress.

The second caveat is the assumption that the dominant vertical mode has a half-wavelength equal to the tropospheric depth. This has been the conventional assumption for many years in studies of tropical dynamics, but Mapes (1993, 2000) has challenged this idea, suggesting that the vertical structure of stratiform rain regions, which have a half-wavelength roughly equal to half the depth of the troposphere, may play a critical role in tropical atmospheric dynamics. If this is so, then we need to completely rethink the basis of the model.

5 Conclusions

The model presented in this paper attempts to make the simplest assumptions about the interaction between deep convective clouds, atmospheric stability and humidity, and radiation which are consistent with our current understanding of the subject. Comparisons with observations and the results of cumulus ensemble models constrain certain model parameters. As a result, the tendency of convection to reduce the effective static stability and thus reduce gravity wave propagation speeds only works for gravity waves with wavelengths greater than the circumference of the earth. The model assumption that the dominant vertical wavelength of convectively coupled disturbances is twice the

depth of the troposphere is crucial to the above conclusions, and needs further examination. In addition, the results need to be extended from the non-rotating case to an equatorial beta-plane.

Acknowledgments. We thank Chris Bretherton for supplying figure 1 of this paper. Chris Bretherton and Jun-Ichi Yano provided insightful reviews of the paper. This work was partially supported by National Science Foundation Grant No. ATM-0079984. In addition, we thank New Mexico Tech president Daniel López and vice president Van Romero for support previous to the commencement of the above grant. The revised version of this paper was completed while the second author was on sabbatical leave at Centro de Ciencias de la Atmósfera, Universidad Autónoma Nacional de México, with support from the University and the Consejo Nacional de Ciencia y Tecnología de México.

6 References

Arakawa, A., and W. H. Schubert, 1974: Interaction of a cumulus cloud ensemble with the large-scale environment, part I. *J. Atmos. Sci.,* **31,** 674-701.

Betts, A. K., 1986: A new convective adjustment scheme. Part I: Observational and theoretical basis. *Quart. J. Roy. Meteor. Soc.,* **112,** 677-691.

Betts, A. K., and M. J. Miller, 1986: A new convective adjustment scheme. Part II: Single column tests using GATE wave, BOMEX, ATEX and arctic air-mass data sets. *Quart. J. Roy. Meteor. Soc.,* **112,** 693-709.

Betts, A. K., and M. J. Miller, 1993: *The Betts-Miller scheme.* The representation of cumulus convection in numerical models, AMS Monograph No. 46, 107-121.

Charney, J. G. and A. Eliassen, 1964: On the growth of the hurricane depression. *J. Atmos. Sci.,* **21,** 68-75.

Cox, S. K., and K. T. Griffith, 1979: Estimates of radiative divergence during Phase III of the GARP Atlantic Tropical Experiment: Part II. Analysis of Phase III results. *J. Atmos. Sci.,* **36,** 586-601.

Emanuel, K. A., 1987: An air-sea interaction model of intraseasonal oscillations in the tropics. *J. Atmos. Sci.,* **44,** 2324-2340.

Emanuel, K., 1993: The effect of convective response time on WISHE modes. *J. Atmos. Sci.,* **50,** 1763-1775.

Emanuel, K. A., J. D. Neelin, and C. S. Bretherton, 1994: On large-scale circulations in convecting atmospheres. *Quart. J. Roy. Meteor. Soc.,* **120,** 1111-1143.

Hayashi, Y. 1971: Large-scale equatorial waves destabilized by convective heating in the presence of surface friction. *J. Meteor. Soc. Japan,* **49,** 458-466.

Lindzen, R. S., 1974: Wave-CISK in the tropics. *J. Atmos. Sci.,* **31,** 156-179.

Madden, R. A., and P. R. Julian, 1994: Observations of the 40-50 day tropical oscillation — a review. *Mon. Wea. Rev.,* **122,** 814-837.

Madden, R., and P. R. Julian, 1971: Detection of a 40-50 day oscillation in the zonal wind in the tropical Pacific. *J. Atmos. Sci.,* **28,** 702-708.

Madden, R., and P. R. Julian, 1972: Description of global-scale circulation cells in the tropics with a 40-50 day period. *J. Atmos. Sci.,* **29,** 1109-1123.

Mapes, B. E., 1993: Gregarious tropical convection. *J. Atmos. Sci.,* **50,** 2026-2037.

Mapes, B. E., 2000: Convective inhibition, subgrid-scale triggering energy, and stratiform instability in a toy tropical wave model. *J. Atmos. Sci.*, **57**, 1515-1535.

Miller, M. J., A. C. M. Beljaars, and T. N. Palmer, 1992: The sensitivity of the ECMWF model to the parameterization of evaporation from the tropical oceans. *J. Climate,* **5,** 418-434.

Neelin, J. D., and J.-Y. Yu, 1994: Modes of tropical variability under convective adjustment and the Madden-Julian oscillation. Part I: Analytical theory. *J. Atmos. Sci.,* **51,** 1876-1894.

Randall, D. A., Harshvardhan, D. A. Dazlich, and T. G. Corsetti, 1989: Interactions among radiation, convection, and large-scale dynamics in a general circulation model. *J. Atmos. Sci.,* **46,** 1943-1970.

Raymond, D. J., 2000a: The Hadley circulation as a radiative-convective instability. *J. Atmos. Sci.,* **57,** 1286-1297.

Raymond, D. J., 2000b: Thermodynamic control of tropical rainfall. *Quart. J. Roy. Meteor. Soc.,* **126,** 889-898.

Raymond, D. J., 2001: A new model of the Madden-Julian oscillation. *J. Atmos. Sci.*, (in press).

Sherwood, S. C., V. Ramanathan, T. P. Barnett, M. K. Tyree, and E. Roeckner, 1994: Response of an atmospheric general circulation model to radiative forcing of tropical clouds. *J. Geophys. Res.,* **99,** 20829-20845.

Slingo, A., and J. M. Slingo, 1988: The response of a general circulation model to cloud longwave radiative forcing. I: Introduction and initial experiments. *Quart. J. Roy. Meteor. Soc.,* **114,** 1027-1062.

Slingo, J. M., and A. Slingo, 1991: The response of a general circulation model to cloud longwave radiative forcing. II: Further studies. *Quart. J. Roy. Meteor. Soc.,* **117,** 333-364.

Tompkins, A. M., and G. C. Craig, 1998: Time-scales of adjustment to radiative-convective equilibrium in the tropical atmosphere. *Quart. J. Roy. Meteor. Soc.,* **124,** 2693-2713.

Wheeler, M., and G. N. Kiladis, 1999: Convectively coupled equatorial waves: analysis of clouds and temperature in the wavenumber-frequency domain. *J. Atmos. Sci.,* **56,** 374-399.

Yamasaki, M., 1969: Large-scale disturbances in a conditionally unstable atmosphere in low latitudes. *Pap. Meteor. Geophys.*, **20**, 289-336.

Yano, J.-I., and K. Emanuel, 1991: An improved model of the equatorial troposphere and its coupling with the stratosphere. *J. Atmos. Sci.,* **48,** 377-389.

7 Figures

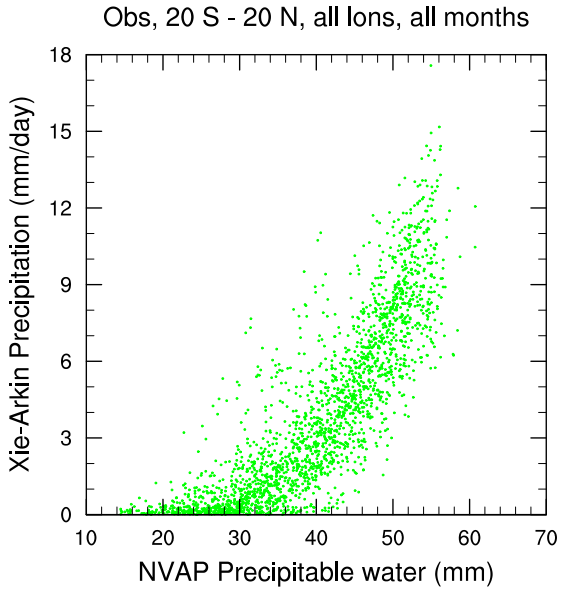

Figure 1: Plot of precipitation rate in the tropics versus precipitable water. Figure courtesy of Chris Bretherton.

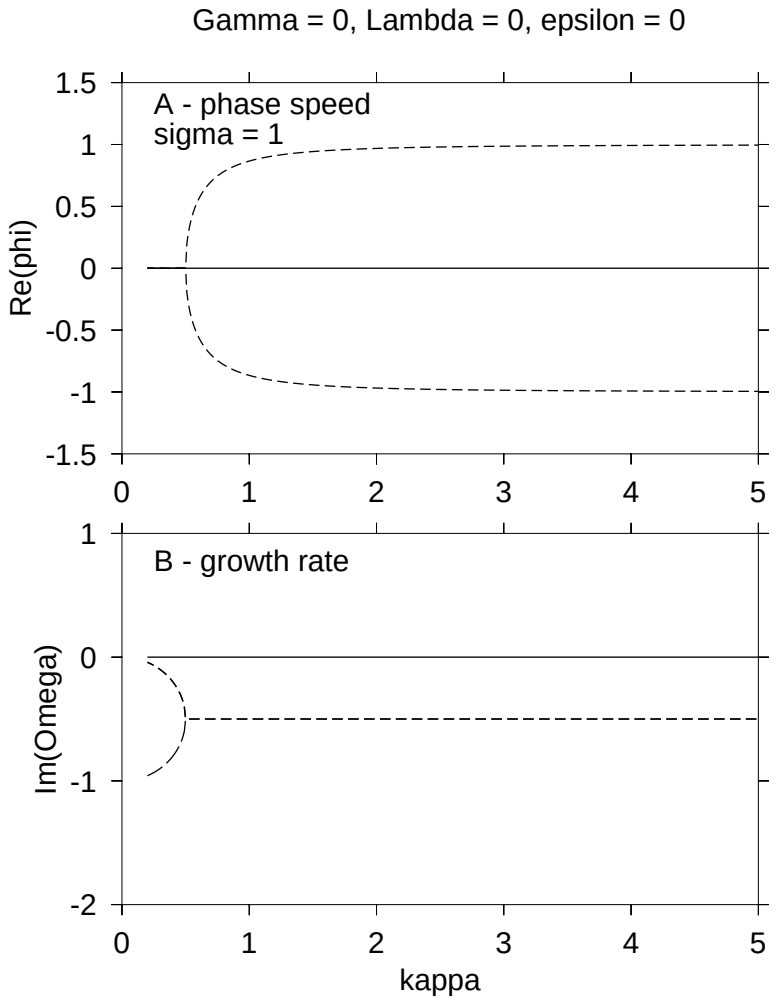

Figure 2: Neutral effective stability with $\sigma = 1$: Dispersion relation for all modes which occur with $\Gamma = 0$, $\Lambda = 0$, and $\epsilon = 0$, presented as (a) the real part of the dimensionless phase speed ϕ and (b) the imaginary part of the dimensionless frequency Ω. Solid, short-dashed, and long-dashed modes correspond between the phase speed and the growth rate panels. Note that solid lines hide dashed lines in some cases.

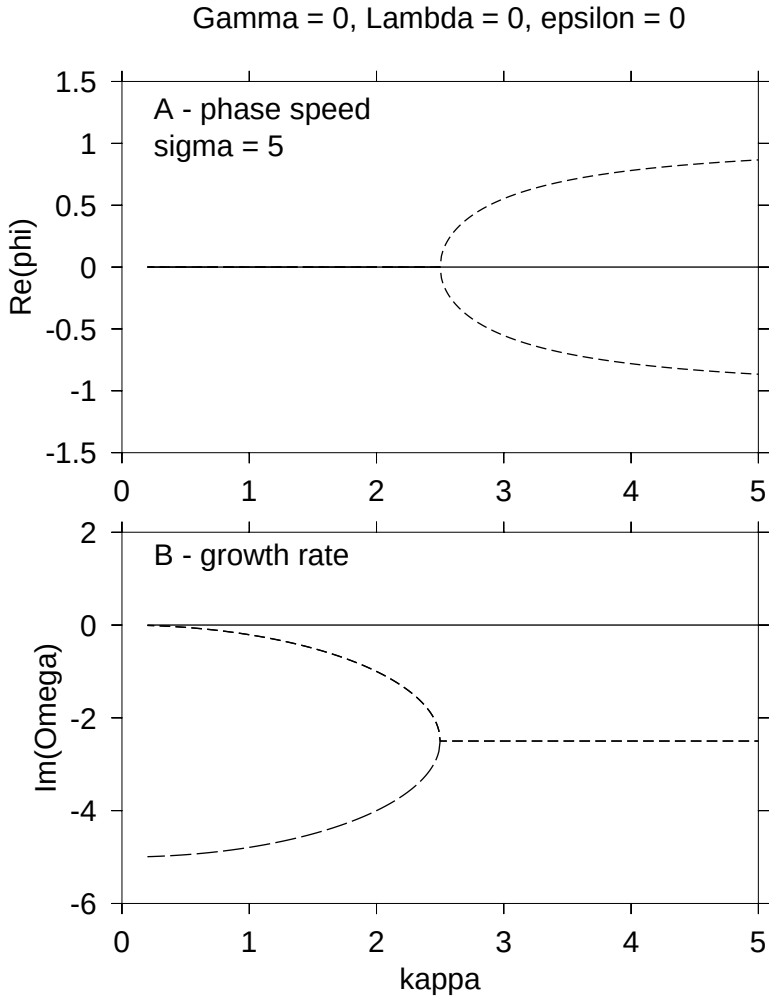

Figure 3: Neutral effective stability with $\sigma = 5$: Otherwise as in figure 2.

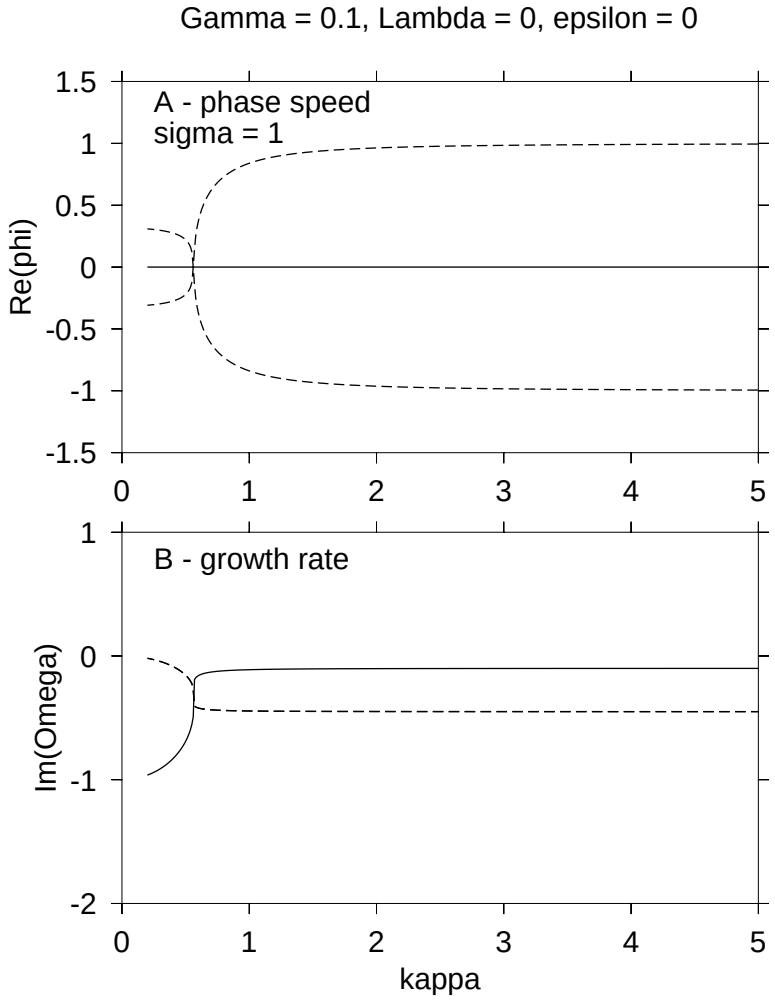

Figure 4: Statically stable with $\Gamma = 0.1$ and $\sigma = 1$: Otherwise as in figure 2.

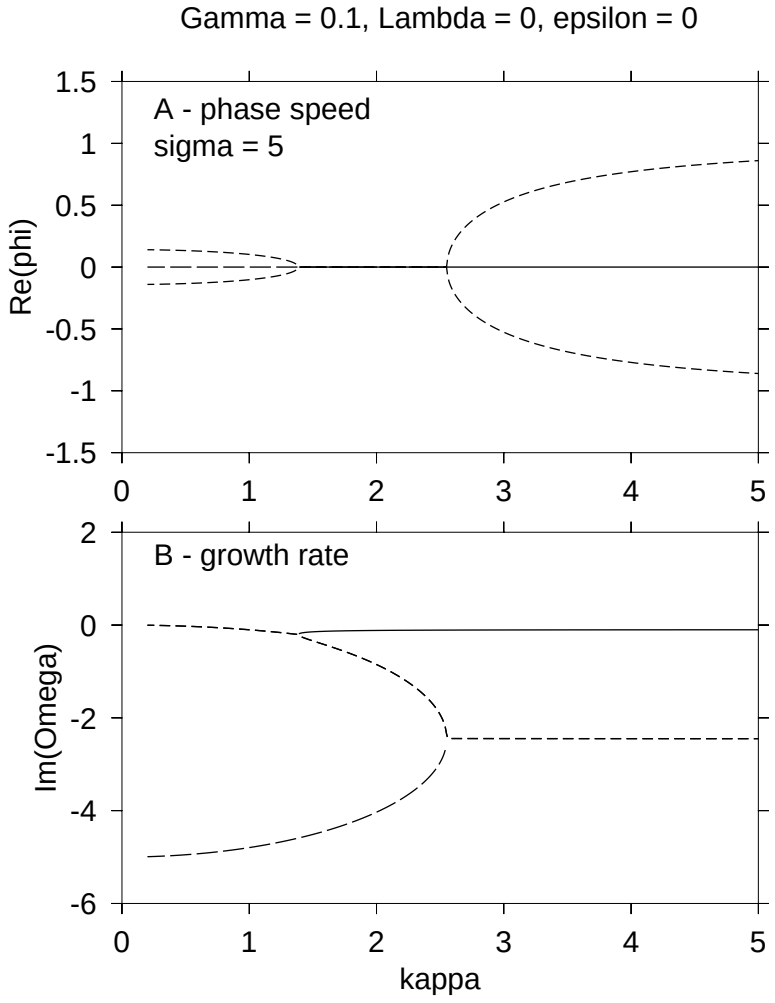

Figure 5: Statically stable with $\Gamma = 0.1$ and $\sigma = 5$: Otherwise as in figure 2.

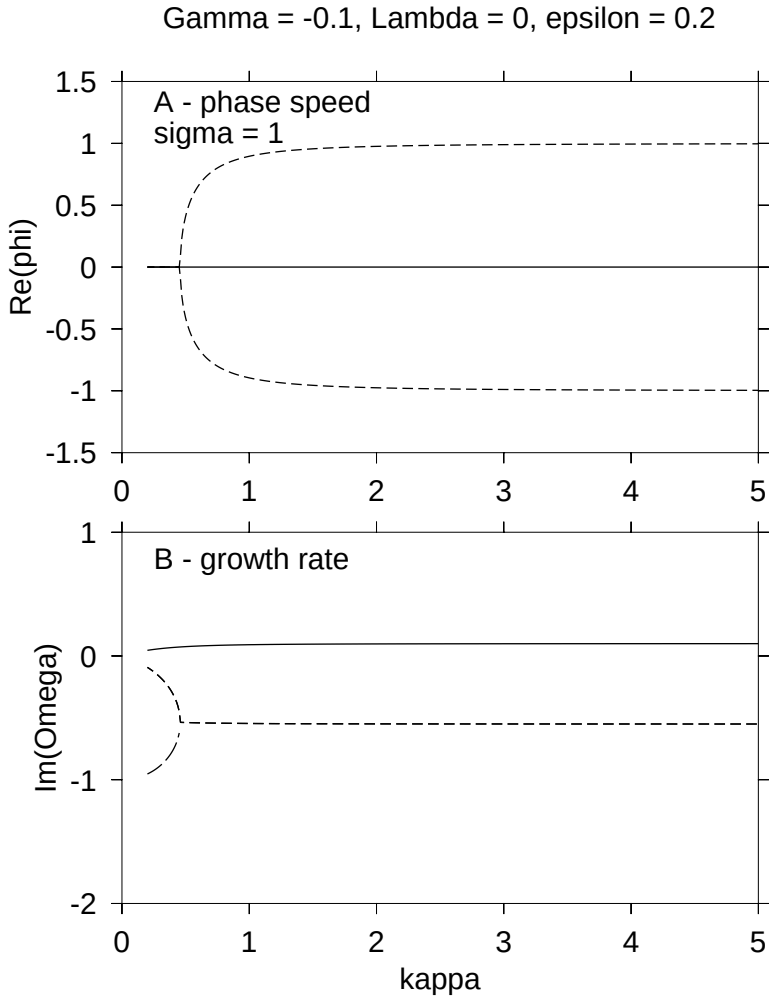

Figure 6: RCI case with $\Gamma = -0.1$, $\epsilon = 0.2$, and $\sigma = 1$: Otherwise as in figure 2.

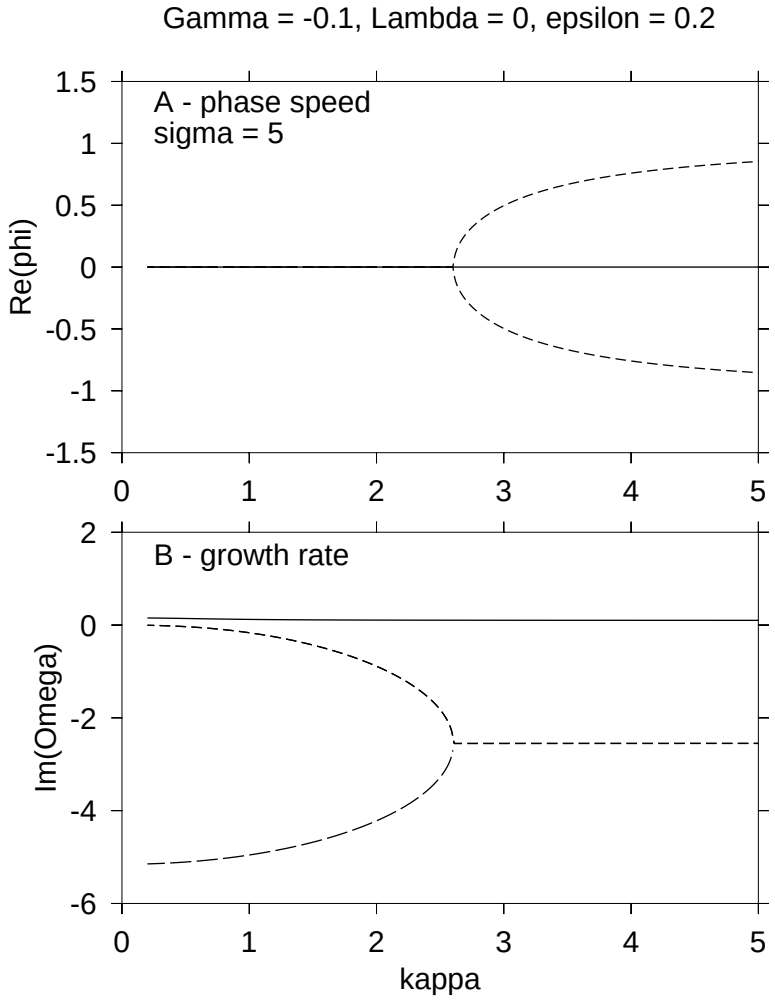

Figure 7: RCI case with $\Gamma = -0.1$, $\epsilon = 0.2$, and $\sigma = 5$: Otherwise as in figure 2.

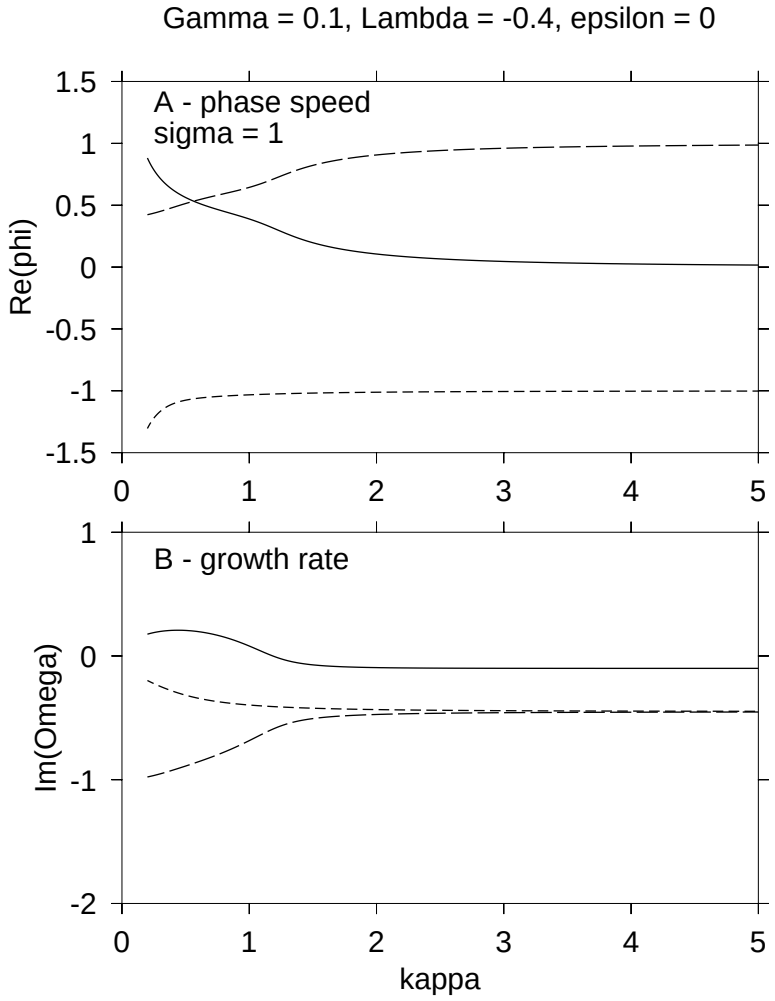

Figure 8: WISHE case with $\Gamma = 0.1$, $\Lambda = -0.4$, and $\sigma = 1$: Otherwise as in figure 2.

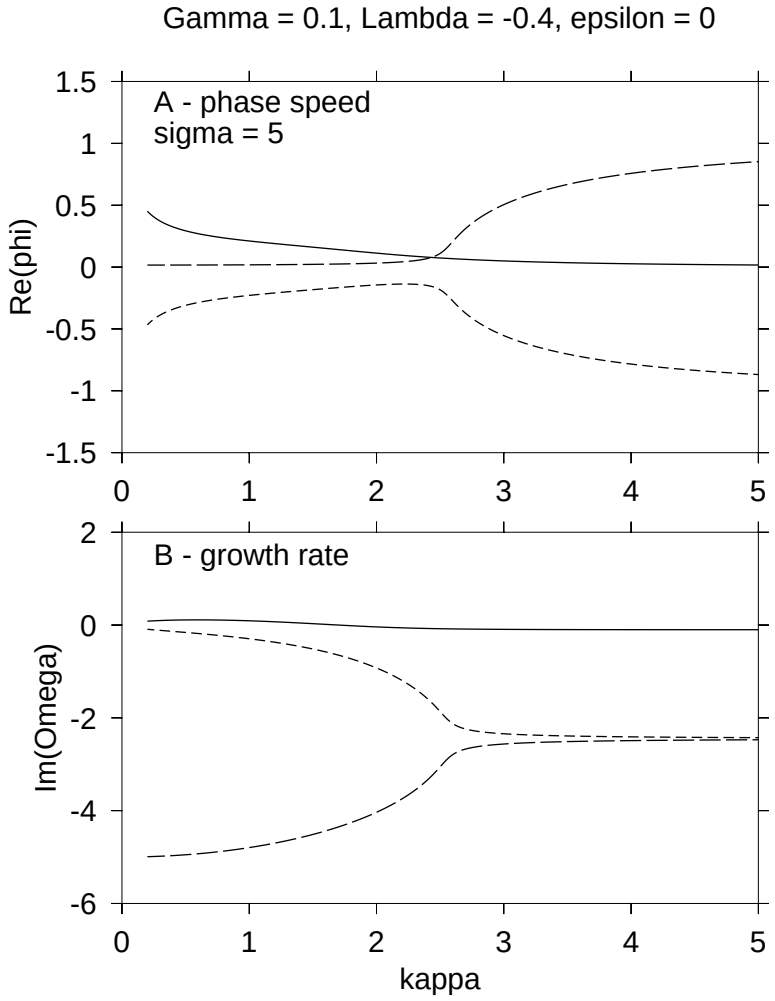

Figure 9: WISHE case with $\Gamma = 0.1$, $\Lambda = -0.4$, and $\sigma = 5$: Otherwise as in figure 2.

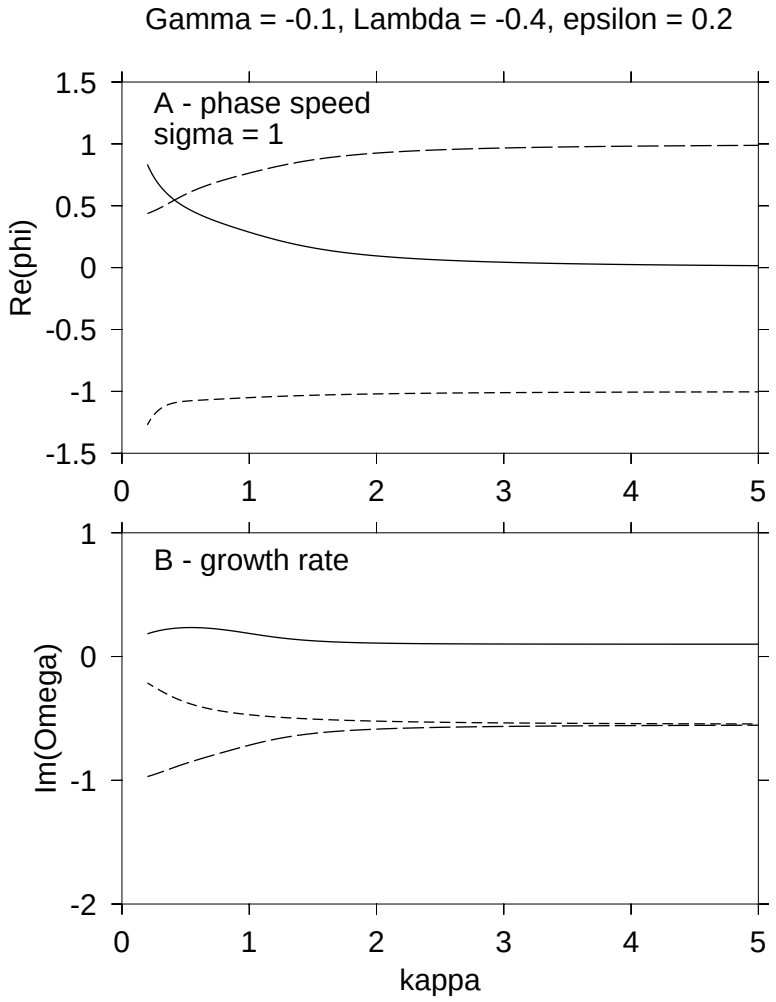

Figure 10: Combined RCI-WISHE case with $\Gamma = -0.1$, $\Lambda = -0.4$, $\epsilon = 0.2$, and $\sigma = 1$: Otherwise as in figure 2.

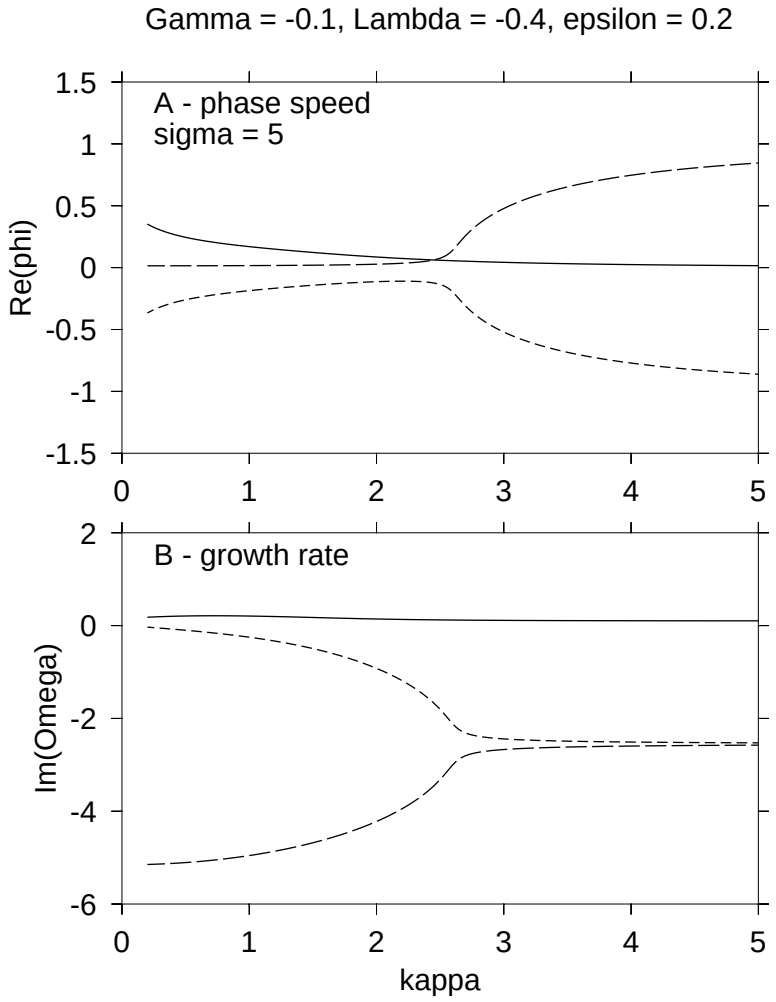

Figure 11: Combined RCI-WISHE case with $\Gamma = -0.1$, $\Lambda = -0.4$, $\epsilon = 0.2$, and $\sigma = 5$: Otherwise as in figure 2.